

Flow characteristics of an inclined air-curtain range hood in a draft

Jia-Kun CHEN¹

¹Institute of Occupational Medicine and Industrial Hygiene, National Taiwan University, Taiwan

Received September 17, 2014 and accepted March 12, 2015

Published online in J-STAGE March 26, 2015

Abstract: The inclined air-curtain technology was applied to build an inclined air-curtain range hood. A draft generator was applied to affect the inclined air-curtain range hood in three directions: lateral ($\theta=0^\circ$), oblique ($\theta=45^\circ$), and front ($\theta=90^\circ$). The three suction flow rates provided by the inclined air-curtain range hood were 10.1, 10.9, and 12.6 m³/min. The laser-assisted flow visualization technique and the tracer-gas test method were used to investigate the performance of the range hood under the influence of a draft. The results show that the inclined air-curtain range hood has a strong ability to resist the negative effect of a front draft until the draft velocity is greater than 0.5 m/s. The oblique draft affected the containment ability of the inclined air-curtain range hood when the draft velocity was larger than 0.3 m/s. When the lateral draft effect was applied, the capture efficiency of the inclined air-curtain range hood decreased quickly in the draft velocity from 0.2 m/s to 0.3 m/s. However, the capture efficiencies of the inclined air-curtain range hood under the influence of the front draft were higher than those under the influence of the oblique draft from 0.3 m/s to 0.5 m/s.

Key words: Kitchen ventilation, Inclined air-curtain, Flow visualization, Draft effect, Capture efficiency

Introduction

Many recent studies have focused on indoor air quality issues in public and residential kitchens^{1–4}. Cooking and cooking burners can emit combustion products, pollutants, and excess moisture that may adversely impact indoor air quality in residences. Especially, frying, grilling, stove use, toasting, etc., can increase the indoor sub-micrometer particle concentration levels and PM_{2.5} concentrations by more than 5 to 90 times higher than normal⁵. Previous studies reported that sub-micrometer particles and chemical compounds generated by cooking or cooking burners resulted in respiratory system problems^{6, 7}. Ventilation

systems play an important role in the energy consumption of heating and cooling, defining the hydrothermal conditions and air quality of dwellings. Among other functions, ventilation systems are necessary to ensure the oxygen levels needed for household combustion appliances⁸. Kitchen ventilation is an important topic in modern building⁹. Exhaust ventilation can be provided via any of the following designs: a range hood or other exhaust devices.

The main purpose of kitchen ventilation is to remove moisture and pollutants from local areas within a house. A range hood, a well-placed wall, or a ceiling exhaust fan can be much more effective than an exhaust fan placed elsewhere in the kitchen or home. Range hoods are important appliances for reducing the amount of cooking-induced harmful materials capable of accumulating in residential sites. The conventional exhaust apparatuses in the kitchens include types of canopy hoods, exterior hoods, and variations. Up-suction, side-suction, and

To whom correspondence should be addressed.
E-mail: jkchen29@ntu.edu.tw

inclined-suction hoods are typical examples. The main structures of a conventional range hood are holes or slots for suction, and fans supply an active pressure gradient for ventilation. The buoyancy force generated by stoves or other heating components and the driving force from blowers or fans, exhaust the contaminant, which includes particles, odors, gases, and heat, outdoors. In a previous study, the capture efficiency was a factor for evaluating the performance of a range hood or a kitchen ventilation system^{10–12}). Some studies reported that the flow visualization technique was used to investigate the airflow around the stove under range hoods¹³). Some studies reported an improvement in kitchen ventilation by modifying kitchen ceilings^{14, 15}). Other studies reported that improving range hoods was a method for controlling pollutants in kitchens. Abanto and Reggio¹⁶) reported that the characteristic curves of a ventilator were built based on numerical results. The hood model has been incorporated into a full-scale kitchen to predict airflow conditions in the space in a kitchen. Yi *et al.*¹²) reported that a concurrent supply and exhaust ventilation system was developed to effectively exhaust heat and contamination from the kitchen. Liu *et al.*¹⁷) reported that air curtains on range hoods control the escape of oil fumes from kitchen hoods. Huang *et al.*¹⁸) investigated the performance of a wall-mounted range hood with laser-assisted flow visualization in static conditions (the draft of the environment was controlled) and dynamic conditions (humans walking by). A novel design of a range hood was reported by Huang *et al.*^{20, 21}). A range hood with the installed inclined air-curtain was called the inclined air-curtain range hood. The inclined air-curtain was installed in front of the range hood to separate the cook and the pollutant generated from the pans of heating oil. For static tests²⁰), the detected tracer-gas concentration of the conventional range hood was larger than that of the air-curtain range hood by about three orders of magnitude around the front edge of countertop. No significant spillages of oil fumes or tracer-gas concentration was observed or detected around the front and lateral planes of the air-curtain range hood. The inclined air-curtain range hood presented excellent hood performance by isolating the oil mists from the mannequin with an air curtain and therefore could reduce spillages out into the atmosphere and the mannequin's breathing zone²¹).

The important parameter affected the performance of the range hoods in kitchens was the uncontrolled draft in the environment. The uncontrolled draft was induced from air conditioners, fans, or the wind got into the space through windows or doors of kitchens. The draft effect was

a kind of continuous disturbance of airflow in kitchens. It was different from the effect of walk-by mentioned by Huang *et al.*^{18, 21}). Chen *et al.*¹⁹) presented the containment of conventional range hoods operating under the effect of a cross draft. When the velocity of the cross draft was greater than 0.2 m/s, the pollutant spillage was increased with the increasing draft velocity.

The performance of the inclined air-curtain range hood was higher than the conventional range hood was represented^{20, 21}). We expected that the performance of the inclined air-curtain range hood was higher than that of the conventional range hoods in the draft effect. We investigated the performance of an inclined air-curtain range hood in a steadily and continuously draft supplied by a homemade draft generator. Using the laser-assisted smoke flow visualization technique and the tracer-gas method, the relation between the flow behaviors and the containment of the inclined air-curtain range hood was studied.

Material and Methods

Experimental space

The test room was a room with dimensions 19 m (length) × 16 m (width) × 5 m (height). The velocity of the environmental draft in the space was less than 5 cm/s. Turbulence and interference from external sources such as an air supply diffuser, doors, and traffic in the room were restricted.

Inclined air-curtain range hood

The inclined air-curtain range hood was assembled with three components: one suction slot, one slot jet, and two guard plates. The stainless-steel suction hood shown in Fig. 1 (a) was installed on the test platform made of aluminum extrusion. The inlet of the suction hood was designed to be a narrow slot 2 cm wide and 70 cm long. In general, entry loss of a slot hood is larger than that of a rectangular opening hood ($W/L > 0.2$, the ratio of width over length of the suction inlet). However, the width of the suction inlet was larger than 14 cm if the $W/L > 0.2$ was adopted. The width of the suction hood was increased to 14 cm so that the area of the inlet of the suction hood was increased. The velocity at the inlet of the suction hood was decreased with the increasing area of the inlet of the suction hood if the suction flow rate was constant. The effective capture velocity was too low to decrease the performance of exhaust the contaminant generated in cooking. Therefore, the width of the inlet of the suction hood was 2 cm ($W/L = 0.028$) for the high capture velocity of the suction hood.

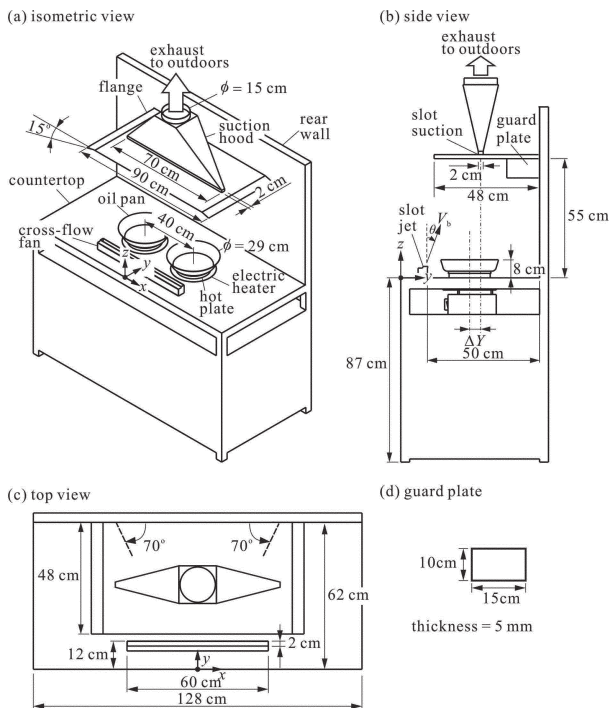


Fig. 1. Configuration of inclined air-curtain range hood. (a) isometric view, (b) side view, (c) top view, (d) guard plate.

The exhaust outlet of the suction hood was a circular hole with a 15 cm diameter. The flange was 48 cm wide and 90 cm long. The flange, which was bent at two sides at a 15° angle, was installed on the inlet of the suction hood. As shown in Fig. 1 (b), the height of the hood was 55 cm in this study.

The slot jet was assembled with three cross-flow fans to form a plan jet. The slot jet was installed 50 cm from the rear wall on the countertop of the test platform. As shown in Fig. 1 (c), the width and length of the slot jet were 2 cm and 60 cm, respectively. According to the result represented by Huang *et al.*²¹⁾, the parameters $V_b=1$ m/s and $\theta=15^\circ$ were suggested that the inclined air-curtain effectively isolated the contaminant from the mannequin. So, the same values of the velocity of the slot jet and the inclined angle of the slot jet shown in Fig. 1 (b) were used in the experiments of the study. The distance ΔY , the offset between the centerline of the suction slot and the centerline of the oil pan, was specified to be 5 cm. The plan jet and the slot suction formed a special flow pattern called the inclined air curtain. The guard plates were 10 cm \times 15 cm rectangular plates made of acrylic. Each guard plate was 5 cm thick. The angle of each installed guard plate on the rear wall was 70°.

The characteristic velocities at the inlet of the suction of

the inclined air-curtain range hood were 12 m/s, 13 m/s, and 15 m/s. The flow rates of the suction velocities were 10.1 m³/min, 10.9 m³/min, and 12.6 m³/min.

Flow visualization

Two electric heaters were installed on the countertop to simulate the burners. Each of the electric heaters was applied 450 W to heat the plate on the heater. The temperature of the hot plate on each electric heater was 360° to 370°. The mineral oil in the oil pans was heated to 210° to 220° by the electric heaters to generate an oil mist for the flow visualization. The diameter of the oil mist droplet, measured with a particle analyzer (Model 2600C, Malvern Instrument Ltd., Malvern, Worcestershire, UK), was 1.7 \pm 0.2 μ m.

A green laser beam with a wavelength of 532 nm was generated from a 100 mW Nd-YAG laser. The laser-light sheet was formed when the laser beam passed through a homemade laser-light expander. The thickness of the laser-light sheet was 0.5 mm. The oil mist generated from heated oil pans scattered the laser light and made the images of the mist in the plane of the laser-light sheet visible. The images were recorded with a charge-coupled device (CCD) camera. The framing rate was 30 frames/s, and the exposure time was 1/60 s.

Draft generator

As shown in Fig. 2 (a), the draft generator consisted of an axial fan, a section of honeycombs, and a section of multi-stage screens. The airflow that exited the axial fan had swirl and fluctuation components. At the exit of the draft generator, the degree of swirl was decreased to a negligibly small value, and the turbulence fluctuation was less than 0.5%. Table 1 shows the nominal draft velocities and the range of centerline velocities within the effective distances. At each rotating speed of the axial flow fan, the centerline velocity values remained somewhat constant at each axial distance from the exit of the draft generator up to some effective distance. Beyond this effective distance, the centerline velocities decayed quickly. We named the persisting centerline velocity before fast decay the “nominal draft velocity,” V_d . The axial distance measured from the exit of the draft generator before the centerline velocity decayed quickly was named the “effective distance.” The draft generator was installed at three locations (lateral $\theta=0^\circ$, oblique $\theta=45^\circ$, frontal $\theta=90^\circ$) to provide a cross draft, as shown in Fig. 2 (b). The horizontal distance between the exit of the draft generator and the center of the countertop was 1 m. The vertical distance from the center

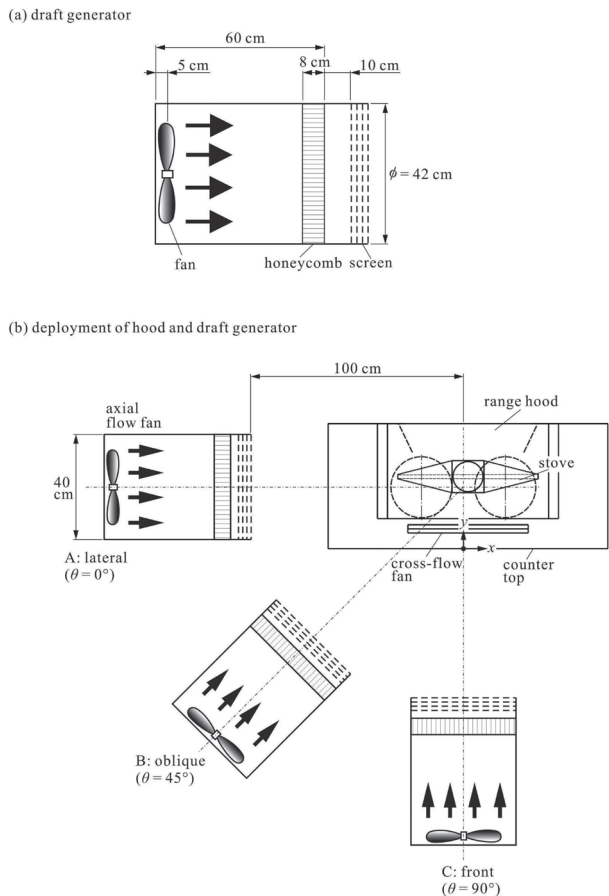


Fig. 2. Draft generator and deployment of draft test. (a) draft generator, (b) deployment of hood and draft generator.

of the draft generator to the surface of the countertop was 0.21 m.

Tracer-gas concentration tests

Sulfur hexafluoride (SF₆) was used as the tracer gas in the experiment. Using the tracer-gas concentration method, the capture efficiency (η) of the inclined air-curtain range hood was evaluated. SF₆ at a concentration of 99.99999% was released from two homemade gas-release rings. As shown in Fig. 3, each homemade gas-release ring, with a diameter of 18 cm, was made of a copper tube. The outer diameter of the copper tube was 0.4 cm, and the copper wall was 0.5 mm thick. Each gas-release ring had 20 holes 0.2 cm in diameter. The flow rate released from each gas-release ring was 3 L/min. The ejected velocity of each hole on the ring was 0.8 m/s. The influence of the tracer-gas jet was negligible in the experiments. The flow was controlled by a homemade system of the flow rate measurement that consisted of a pressure gauge, a needle valve, and a calibrated rotameter. The gas-release rings were attached

Table 1. Nominal velocity (V_d) of draft generator

Nominal draft velocity V_d (m/s)	Effective distance (m)	Velocity range (m/s)
0.1	0.80–1.03	0.09–0.13
0.2	0.08–1.06	0.19–0.20
0.3	0.75–1.00	0.27–0.32
0.4	0.07–1.10	0.39–0.41
0.5	0.60–1.07	0.48–0.50
0.6	0.75–1.30	0.57–0.61
0.7	0.35–1.40	0.70–0.72

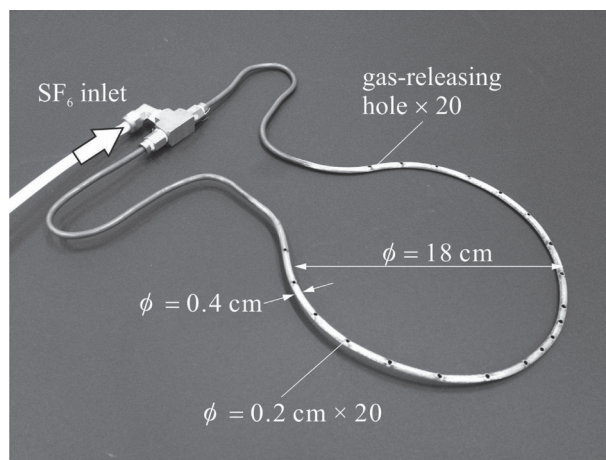


Fig. 3. Sulfur hexafluoride gas-release ring.

to the hot plates (which were heated to 380 °C) of the electric heaters so that the SF₆ gas would receive heat and buoyancy from the hot plates. A Miran SapphIRe Portable Ambient Analyzer (Thermo Electron Corp., Franklin, MA, USA) was used to measure the concentration of SF₆ gas. The resolution of the analyzer was 0.001 ppm for measurement of the concentration of SF₆ gas, and the sampling rate was 20 readings per second.

For the static condition (i.e., the velocity of the airflow in the space was controlled at slower than 5 cm/s), the definition of the capture efficiency was the ratio of the contaminants captured by the hood to the total contaminants produced at the source²²). Two gas-release rings were inserted into the suction slot of the inclined air-curtain range hood to ensure that the total released SF₆ was injected into the piping system. The total flow rate of SF₆ from the two gas-release rings was 6 L/min for 12 min. The SF₆ concentration was measured at the location about 1.0 m upstream of the end of the piping system (20 m long).

As shown in Fig. 4, the average value over $t=t_4-t_3$ is denoted as C_1 . The average value over time $t=t_2-t_1$ is

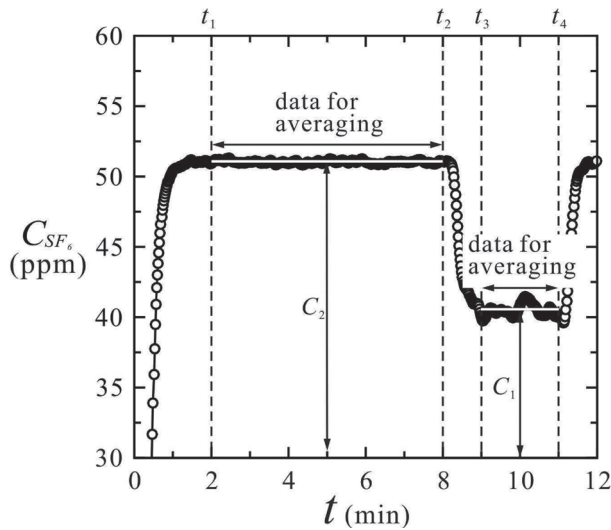


Fig. 4. Typical time history of SF₆ gas concentration detected at exhaust pipe of range hood for capture index measurement.

denoted as C_2 . The capture efficiency η is calculated by

$$\eta = \frac{C_1}{C_2} \times 100\% \quad (1)$$

For the draft condition, the measurement method for C_2 was the same as that of the static condition; however, the measurement of C_1 was a little different. The gas-release rings were placed on the hot plates of the electric heaters, and the SF₆ concentration in the exhaust pipe was measured from time zero for 12 min. During the lead-in period of 8 min, the draft was not applied; the draft was then applied for the next 3 min and stopped at $t=11$ min. The typical time-varying SF₆ concentration for transition from the “no draft” to the “draft” condition is shown in Fig. 4. When the draft was applied at $t=8$ min, the SF₆ concentration dropped quickly within 1 min and fluctuated in terms of a low time-averaged level C_1 . After the draft was stopped at $t=11$ min, the SF₆ concentration recovered to normal values at $t > 11.5$ min.

Results and Discussion

In the study reported by Huang *et al.*²⁰⁾, the flow formed by the oil mist generated by heating the oil pans on the countertop was restricted stably within the range between the guard plates in a test under static conditions.

The laser-light sheet shown in Fig. 5 was located at the plane of $z=40$ cm, and the distribution of the oil mist was formed by the effect of the draft velocity of 0.2 m/s from three directions. The results showed that $V_d=0.2$ m/s was

too weak to affect the flow structure of the inclined air-curtain range hood. However, the variations of the oil mist distribution were observed with the different directions of the draft effect. When the draft blown from the lateral direction ($\theta=0^\circ$), there was no air curtain to resist the draft in the lateral direction so that the oil mist was moved to the right of Fig. 5 (a). When the draft blown from the oblique direction ($\theta=45^\circ$), some part of the draft was resisted by the inclined air-curtain so that the oil mist was moved toward the rear wall and the right of Fig. 5 (c). When the draft blown from the front direction ($\theta=90^\circ$), the draft was resisted by the inclined air-curtain. Although, the draft was resisted by the inclined air-curtain, the oil mist was pushed by the airflow came from the front direction. Therefore, it was observed that the oil mist was moved toward the rear wall of the range hood. When the suction flow rate was increased, the obvious improvement of the oil mist distribution was shown in Fig. 5 (b).

As shown in Fig. 6, for the draft velocity 0.3 m/s, the flow structure was different from that in Fig. 5. The dispersion zone of the oil mist in Fig. 5 was expanded, especially in Fig. 6 (c), 6 (d), and 6 (e). At the 0.3 m/s draft velocity, the flow of the oil mist was dispersed at a low flow rate, i.e., $Q_s=10.1$ m³/min. The increased draft velocity from the lateral direction ($\theta=0^\circ$) forced the oil mist to move to the right, as shown in Fig. 6 (a), when the flow rate of the range hood was 10.1 m³/min. When the flow rate was increased to 12.6 m³/min, the oil mist shown in Fig. 6 (b) was stably restricted under the hood. When the draft was applied from the oblique direction ($\theta=45^\circ$), the oil mist, shown in Fig. 6 (c), was dispersed, and the zone of the oil mist was larger than that shown in Fig. 5 (c). When the draft was applied from the oblique direction, the oil mist was attached to the rear wall, and the right part of the oil mist moved to an area close to the edge of the flange of the range hood. The compact structure of the oil mist, as shown in Fig. 5 (d), was destroyed to disperse slightly, as shown in Fig. 6 (d), due to the draft velocity of 0.3 m/s even if the oil mist was still restricted under the range hood. When the front draft ($\theta=90^\circ$) was applied, the flow of the oil mist, shown in Fig. 6 (e), moved to attach on the rear wall of the range hood at a low flow rate of 10.1 m³/min. The flow, shown in Fig. 6 (f), was stable at the 12.6 m³/min flow rate.

The draft velocity increased to 0.5 m/s, as shown in Fig. 7. As shown in Fig. 7 (a) and 7 (b), the oil mist dispersed to the right side and leaked out of the flange when the draft was applied from the direction of $\theta=0^\circ$ even though the flow rate was increased to 12.6 m³/min. When

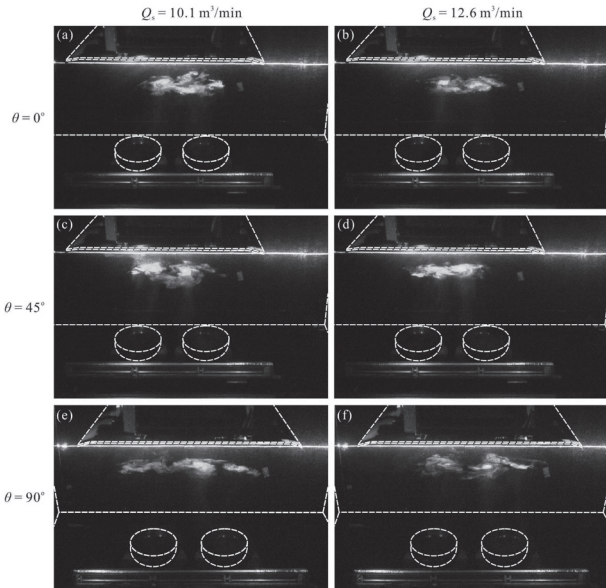


Fig. 5. Images of oil mist in horizontal plane at $z=40$ cm. $V_d=0.2$ m/s. (a) $Q_s=10.1$ m³/min and $\theta = 0^\circ$, (b) $Q_s=12.6$ m³/min and $\theta=0^\circ$, (c) $Q_s=10.1$ m³/min and $\theta=45^\circ$, (d) $Q_s=12.6$ m³/min and $\theta=45^\circ$, (e) $Q_s=10.1$ m³/min and $\theta=90^\circ$, (f) $Q_s=12.6$ m³/min and $\theta=90^\circ$.

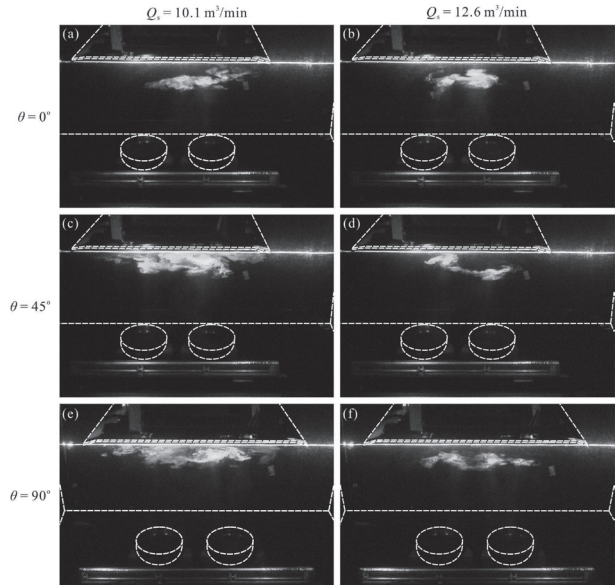


Fig. 6. Images of oil mist in horizontal plane at $z=40$ cm. $V_d=0.3$ m/s. (a) $Q_s=10.1$ m³/min and $\theta=0^\circ$, (b) $Q_s=12.6$ m³/min and $\theta=0^\circ$, (c) $Q_s=10.1$ m³/min and $\theta = 45^\circ$, (d) $Q_s=12.6$ m³/min and $\theta=45^\circ$, (e) $Q_s=10.1$ m³/min and $\theta=90^\circ$, (f) $Q_s=12.6$ m³/min and $\theta=90^\circ$.

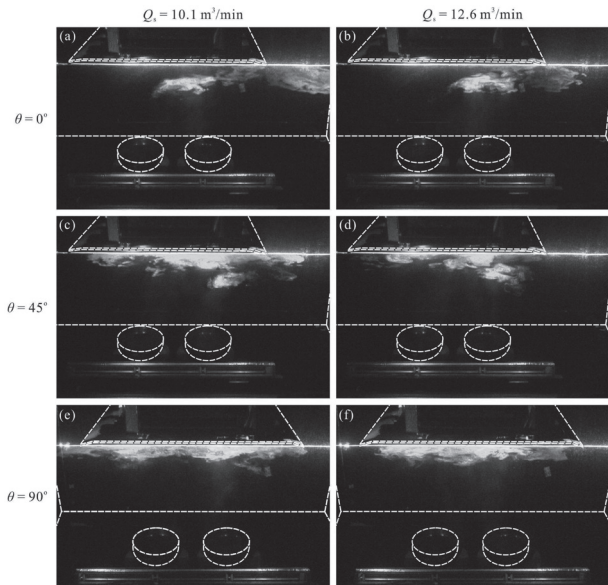


Fig. 7. Images of oil mist in horizontal plane at $z=40$ cm. $V_d=0.5$ m/s. (a) $Q_s=10.1$ m³/min and $\theta=0^\circ$, (b) $Q_s=12.6$ m³/min and $\theta=0^\circ$, (c) $Q_s=10.1$ m³/min and $\theta=45^\circ$, (d) $Q_s=12.6$ m³/min and $\theta=45^\circ$, (e) $Q_s = 10.1$ m³/min and $\theta=90^\circ$, (f) $Q_s=12.6$ m³/min and $\theta=90^\circ$.

the applied draft was in the direction of $\theta=45^\circ$, the containment of the flow rate of 12.6 m³/min was better than that of the flow rate of 10.1 m³/min. Although the higher flow rate was used, leakage was found around the front of the flange, as shown in Fig. 7 (d). As shown in Fig. 7 (e),

the flow rate of 10.1 m³/min was too low to restrict the oil mist even though there was an inclined air curtain in front of the range hood. However, the oil mist, shown in Fig. 7 (f), was restricted under the area of the flange of the range hood at the flow rate of 12.6 m³/min when the draft velocity 0.5 m/s was applied in the front direction.

Figure 8 shows the capture efficiency η varying with the draft velocity V_d . For the cases of $\theta=0^\circ$, the variation of η decreased rapidly when V_d varied from 0.2 m/s to $V_d=0.3$ m/s. In Fig. 8, the capture efficiency was little changed for the cases of $\theta=45^\circ$ in the section of the draft of 0.2 m/s to 0.3 m/s. When the draft velocity was higher than 0.3 m/s, the capture efficiency of the range hood decreased an average of 18.8% when the draft velocity increased from 0.3 m/s to 0.4 m/s. As shown in Fig. 8, the trend of the cases of $\theta=90^\circ$ changed moderately in the range from 0.2 m/s to 0.4 m/s and changed rapidly in the range from 0.4 m/s to 0.5 m/s. For the cases of $\theta=90^\circ$, the variation of the capture efficiency in the three flow rates was a maximum of 2%, when the draft velocity was in the section from 0.2 m/s to 0.4 m/s. However, the variation increased 8.6% on average when the draft velocity increased from 0.4 m/s to 0.5 m/s.

As shown in Fig. 8, the draft effect began to be active to the inclined air-curtain range hood was the draft velocity of 0.3 m/s. In the draft velocity of 0.3 m/s, the capture efficiency of the cases of $\theta=0^\circ$ was lowest among the

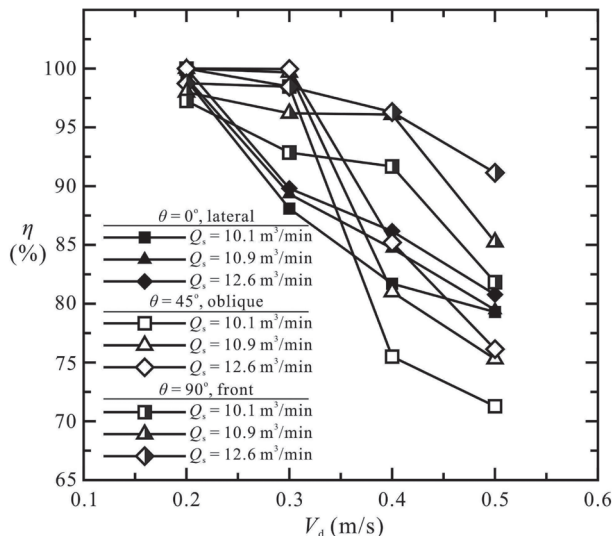


Fig. 8. Capture efficiencies of inclined air-curtain range hood with respect to influences of draft from various directions and suction flow rates.

draft effect of the three directions. In the case of $\theta=45^\circ$, the maximum of the variation of the capture efficiency was recorded in the range from 0.3 m/s to 0.4 m/s. For all cases, the increased suction flow rate was efficient for the containment of the inclined air-curtain range hood. Especially, the capture efficiency was higher than 90% in the effect of the draft velocity of 0.5 m/s when the suction flow rate was 12.6 m³/min in the case of $\theta=90^\circ$.

To compare the results represented by Chen *et al.*¹⁹⁾, the performances of the conventional and jet-isolated range hoods were obviously decreased when the draft velocity was higher than 0.3 m/s. The same result shown in Fig. 8 was found on the inclined air-curtain range hood. When the draft velocity was 0.3 m/s in any direction of the three directions, the capture efficiencies of the inclined air-curtain range hood and the conventional range hood were on the same level in 12.6 m³/min of the suction flow rate. When the draft velocity was lower than 0.3 m/s in any direction of the three directions, the capture efficiency of the inclined air-curtain range hood was higher than that of the conventional range hood in 12.6 m³/min of the suction flow rate. In the oblique and front directions, the capture efficiency of the inclined air-curtain range hood in 12.6 m³/min of the suction flow rate was higher than that of the jet-isolated range hood in 15.0 m³/min of the suction flow rate when the draft velocity was smaller than 0.3 m/s.

Conclusions

The containment ability of the inclined air-curtain range hood was tested in the draft effect. The capture efficiency was the index to evaluate the performance of the containment of the range hood. From the results, low capture efficiency was observed when the draft effect was applied from the lateral direction. High capture efficiency was observed when the draft effect was applied from the front direction. If the draft effect was applied from the oblique direction, the capture efficiency of the inclined air-curtain range hood did not decrease at a draft velocity less than 0.4 m/s. Increasing the suction flow rate of the hood was efficient to improve the capture efficiency of the inclined range hood. The capture efficiency was higher than 90% at the flow rate of 12.6 m³/min and the draft velocity of 0.5 m/s in the case of $\theta=90^\circ$. Using air-curtain technology, the capture efficiency became low at the draft velocity higher than 0.5 m/s. The draft effect in a kitchen affects the air quality in that room. The results of the study pointed out that the containment ability of the inclined air-curtain range hood was weak when the draft came from the lateral direction. The containment ability of the inclined air-curtain range hood was strong when the draft came from the front direction.

Acknowledgement

The authors gratefully acknowledge the financial support provided to this study by the National Science Council of Taiwan under Grant No. NSC 102-2221-E-011-053.

References

- 1) Chowdhury Z, Le LT, Masud AA, Chang KC, Alauddin M, Hossain M, Zakaria ABM, Hopke PK (2012) Quantification of indoor air pollution from using cookstoves and estimation of its health effects on adult women in northwest Bangladesh. *Aerosol Air Qual Res* **12**, 463–75.
- 2) Saha S, Guha A, Roy S (2012) Experimental and computational investigation of indoor air quality inside several community kitchens in a large campus. *Build Environ* **52**, 177–90.
- 3) Li A, Zhao Y, Jiang D, Hou X (2012) Measurement of temperature, relative humidity, concentration distribution and flow field in four typical Chinese commercial kitchens. *Build Environ* **56**, 139–50.
- 4) Gao J, Cao C, Zhang X, Luo Z (2013) Volume-based size distribution of accumulation and coarse particles (PM_{0.1–10}) from cooking fume during oil heating. *Build Environ* **59**, 575–80.

- 5) He C, Morawska L, Hitchins J, Gilbert D (2004) Contribution from indoor sources to particle number and mass concentrations in residential houses. *Atmos Environ* **38**, 3405–15.
- 6) Svendsen K, Sjaastad AK, Sivertsen I (2003) Respiratory symptoms in kitchen workers. *Am J Ind Med* **43**, 436–9.
- 7) Sisti J, Boffetta P (2012) What proportion of lung cancer in never-smokers can be attributed to known risk factors? *Int J Cancer* **131**, 265–75.
- 8) Pinto M, Viegas J (2013) The influence of ventilation systems on domestic gas appliances: an experimental study. *Build Environ* **69**, 1–13.
- 9) Lee H, Lee YJ, Park SY, Kim YW, Lee Y (2012) The improvement of ventilation behaviours in kitchens of residential buildings. *Indoor Built Environ* **21**, 48–61.
- 10) Li Y, Delsante A, Symons J (1997) Residential kitchen range hoods—buoyancy-capture principle and capture efficiency revisited. *Indoor Air* **7**, 151–7.
- 11) Zhao YJ, Li AG, Tao PF, Gao R (2013) The impact of various hood shapes, and side panel and exhaust duct arrangements, on the performance of typical Chinese style cooking hoods. *Build Simul-China* **6**, 139–49.
- 12) Delp WW, Singer BC (2012) Performance assessment of U.S. residential cooking exhaust hoods. *Environ Sci Technol* **46**, 6167–73.
- 13) Hargather MJ, Settles GS (2011) Background-oriented schlieren visualization of heating and ventilation flows: HVAC-BOS. *HVAC R Res* **17**, 771–80.
- 14) Kosonen R, Mustakallio P (2003) The influence of a capture jet on the efficiency of a ventilated ceiling in a commercial kitchen. *Int J Vent* **1**, 189–99.
- 15) Kosonen R (2007) The effect of supply air systems on the efficiency of a ventilated ceiling. *Build Environ* **42**, 1613–23.
- 16) Abanto J, Reggio M (2006) Numerical investigation of the flow in a kitchen hood system. *Build Environ* **41**, 288–96.
- 17) Liu X, Wang X, Xi G (2014) Orthogonal design on range hood with air curtain and its effects on kitchen environment. *J Occup Environ Hyg* **11**, 186–99.
- 18) Huang RF, Dai GZ, Chen JK (2010) Effects of mannequin and walk-by motion on flow and spillage characteristics of wall-mounted and jet-isolated range hoods. *Ann Occup Hyg* **54**, 625–39.
- 19) Chen JK, Huang RF, Peng KL (2012) Flow characteristics and spillage mechanisms of wall-mounted and jet-isolated range hoods subject to influence from cross draft. *J Occup Environ Hyg* **9**, 36–45.
- 20) Huang RF, Nian YC, Chen JK (2010) Static condition differences in conventional and inclined air-curtain range hood flow and spillage characteristics. *Environ Eng Sci* **27**, 513–22.
- 21) Huang RF, Nian YC, Chen JK, Peng KL (2011) Improving flow and spillage characteristics of range hoods by using an inclined air-curtain technique. *Ann Occup Hyg* **55**, 164–79.
- 22) Li Y, Delsante A (1996) Derivation of capture efficiency of kitchen range hoods in a confined space. *Build Environ* **31**, 461–8.